

# ELECTROMECHANICAL BEHAVIOUR OF PIT Nb<sub>3</sub>Sn WIRES FOR NED\*

B. Seeber, C. Senatore, F. Buta and R. Flükiger, University of Geneva-GAP, Geneva, Switzerland  
T. Boutboul, C. Scheuerlein, L. Oberli and L. Rossi, CERN, Geneva, Switzerland

## Abstract

The critical current vs. axial tensile strain and transverse compressive force for two PIT Nb<sub>3</sub>Sn conductors, manufactured by SMI (now EAS), has been investigated. In addition, the distribution of the critical temperature has been determined by specific heat measurements. After identical reaction heat treatments wire #B207 has a slightly broader  $T_c$  distribution than wire #B215 and less volume fraction of Nb<sub>3</sub>Sn. The behaviour under axial tensile strain is as expected, although the strain for maximum current,  $\epsilon_m$ , is relatively low. However the studied wires are rather sensitive to transverse compressive forces. For instance at 10 kN and 15 T the critical current is reduced to 48% of its initial value and recovers only partially after unloading.

## INTRODUCTION

For the construction of superconducting magnets the knowledge of the strand characteristics is important. In the case of Nb<sub>3</sub>Sn, which is particularly sensitive to mechanical loads, detailed data on the critical current vs. axial tensile/compressive strain as well as under transverse compressive stress are requested. This information is especially needed where the limits of the superconductor are approached, e.g. for high field dipole magnets like NED (Next European Dipole).

The studied Nb<sub>3</sub>Sn PIT conductors, produced by SMI (now EAS), are candidates for NED. They are designed for an optimum critical current at the required field but no measures have been taken so far for mechanical reinforcement. In the first part of this paper the critical current as a function of axial tensile strain at different fields is presented. In the second part the critical current vs. transverse compressive force at various fields is reported. Finally the response to mechanical loads on these PIT wires is compared to that of a Nb<sub>3</sub>Sn bronze route wire.

## SAMPLE CHARACTERISTICS

The investigated PIT wires have been manufactured by SMI (now EAS). Both samples, #B207 and #B215, have an almost identical layout with a nominal OD of 1.25 mm, 288 Nb/Nb<sub>3</sub>Sn filaments with a diameter of about 50  $\mu$ m and a twist pitch length of 20 mm. The Cu/non-Cu area is slightly different and the quality of the powder is lower for wire #B207 (for unknown reasons). A micrograph of #B207 can be seen in Fig. 1 while the most important characteristics are summarized in Table I. After the reaction heat treatment at 675°C for 84 hours, the

values of the residual resistivity ratio,  $RRR$ , measured according to IEC 61788-11, were relatively high (Table I). They present an average over two and six measurements for wire #B207 and #B215, respectively.

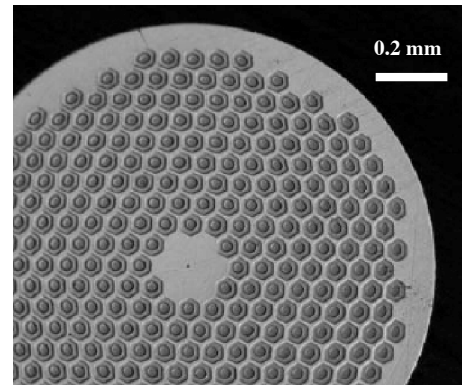


Figure 1. Micrograph of the investigated PIT wires #B207 with 288 hexagonal filaments of about 50  $\mu$ m in size.

TABLE I. CHARACTERISTICS OF THE STUDIED Nb<sub>3</sub>Sn WIRES

Strand ID	PIT #B207	PIT #B215
Size (mm)	Ø 1.25	Ø 1.25
Number of filaments	288	288
Filament size ( $\mu$ m)	~ 50	~ 50
Filament twist pitch (mm)	20	20
Cu / non-Cu area	0.96	1.22
Reaction heat treatment (vacuum)	675°C/84h	675°C/84h
Residual resistance ratio – RRR	195	211

## RESULTS

### Calorimetric $T_c$ distribution

In order to investigate the superconducting properties over the whole wire volume, we have developed a method of analysis based on specific heat measurements. In fact, any gradient in the Sn content causes a distribution of  $T_c$  in the wire. Since this distribution cannot be determined by conventional techniques, due to percolation and/or magnetic shielding effects, a particular deconvolution method of the specific heat data was developed, allowing the determination of the precise distribution of  $T_c$  in multifilamentary Nb<sub>3</sub>Sn wires [1]. A further advantage of this technique is the possibility of performing the

\*This work was supported in part by the Swiss National Science Foundation through the National Centre of Competence in Research, "Materials with Novel Electronic Properties, MANEP" and by CERN.

measurements in the presence of the matrix, i.e. under thermal pre compression.

The specific heat for wire #B207 and #B215 was measured from 2 to 25 K at zero field and at 14 T, applying a long relaxation technique [2]. A CERNOX chip was used both as sample holder and as thermometer/heater.

In order to separate the superconducting transition of the filaments from the background of phonons and normal electrons, the specific heat of the normal state has been subtracted for each sample from the curve measured at zero field. The specific heat of the normal state in the temperature range 2-20 K has been determined from the data above the superconducting transition measured at high field. In particular the data above 13 K have been fitted according to the law  $c_{fit}(T) = \gamma T + \beta_3 T^3 + \beta_5 T^5$  by imposing the conservation of the entropy, i.e.

$$\int_0^{20\text{K}} \frac{c_{fit}(T)}{T} dT = \int_0^{20\text{K}} \frac{c(T, B=0)}{T} dT \quad (1)$$

The superconducting transitions detected by specific heat for the two wires are illustrated in Fig. 2. The transition corresponding to the unreacted Nb is also present.

The height of the specific heat anomaly at the superconducting transition is directly related to the gap energy of the superconductor. Since the specific heat curves in Fig. 2 have been normalized to the total mass of the wires (Cu + filaments), the height of the anomaly provides an estimation of the relative A15 amount in the different samples. In particular wires #B207 and #B215 exhibit the same onset  $T_c$  but the superconducting jump is higher for wire #B215, indicating a higher amount of A15 phase ( $\sim 5\%$ ). The Sn composition gradient inside the filaments determines the broadening of the superconducting transition. Note that at zero field, the onset of the superconducting transition of the A15 filaments is well above 18 K, due to the addition of Ta in

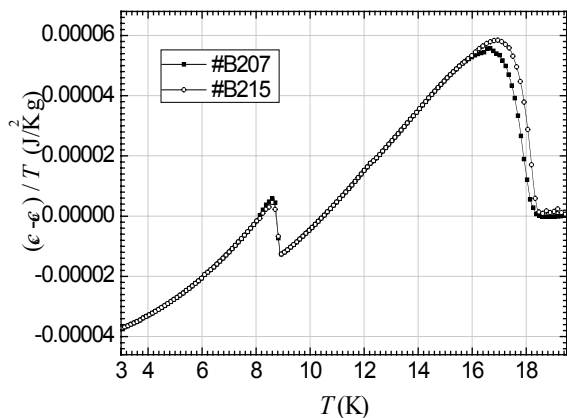


Figure 2. Specific heat for the superconducting volume of wire #B207 (solid squares) and #B215 (open circles); around 9 K the superconducting transition of the unreacted Nb it is clearly visible.

the Nb tubes. An increase of  $T_c$  with respect to the value for pure  $\text{Nb}_3\text{Sn}$  was already reported by Suenaga et al. [3].

The  $T_c$  distributions obtained from the model in Ref.[1] are reported in Fig. 3. The temperature corresponding to the maximum of the distribution is higher in the case of wire #B215, thus indicating a smaller Sn gradient and a slightly higher Sn content in the A15 layer of wire #B215 with respect to wire #B207.

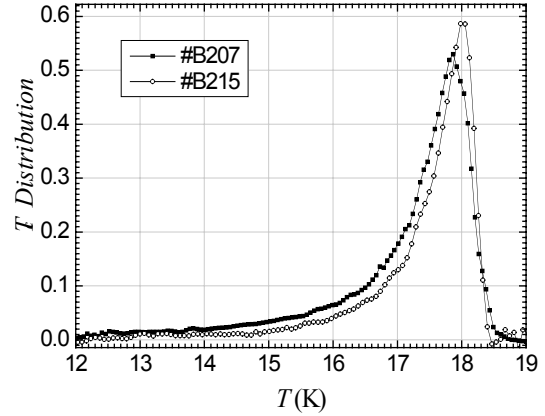


Figure 3.  $T_c$  distribution in wires #B207 (solid squares), #B215 (open circles), obtained by the deconvolution of

### Critical current vs. axial tensile strain

The dependence of the critical current under axial tensile strain was investigated with our Walters spring probe [4]. For this purpose the superconducting wire is mounted on the Walters spring in a precisely machined groove. An intentional axial backlash allows the wire to be cooled down in the strain free state. Then the critical current for zero strain is measured at the highest available field (reduced Lorentz force) by rotating the spring in the tensile direction until an increase of  $I_c$  is detected. After warming up to room temperature, the superconducting wire is soldered over its total length. Finally the probe is cooled to 4.2 K a second time and the critical current for zero applied strain can be found by rotating the Walters spring in the appropriate direction. This process requires a reversible  $I_c$  behaviour in the considered strain window, which is normally the case.

Fig. 4 summarizes the measurements at different magnetic fields up to 21 T, the maximum available field in our laboratory. Data below 15 T are not available due to the limitation of the sample current power supply of 1000 A. Due to quench problems at the current terminals of wire #B215 at 15 T, data points near the maximum of the critical current could not be obtained. However, two points could be measured at higher strain allowing a fit to the data. In general, the  $I_c$  values for wire #B207 are considerably lower in comparison to those of #B215. There is also a shift of the strain position for maximum  $I_c$ ,  $\epsilon_m$ , from 0.14% to 0.18%, indicating a higher thermal prestrain for wire #B215.

The reversibility of  $I_c$  upon unloading has also been studied for wire #B215 at 19 T (Fig. 4c). The critical current, as well as the  $n$  value recover completely until a tensile strain of 0.31%. Further loading to 0.36% revealed a partial damage of the wire so the irreversibility limit,  $\epsilon_{irr}$ , is situated in the range between 0.31% and 0.36%

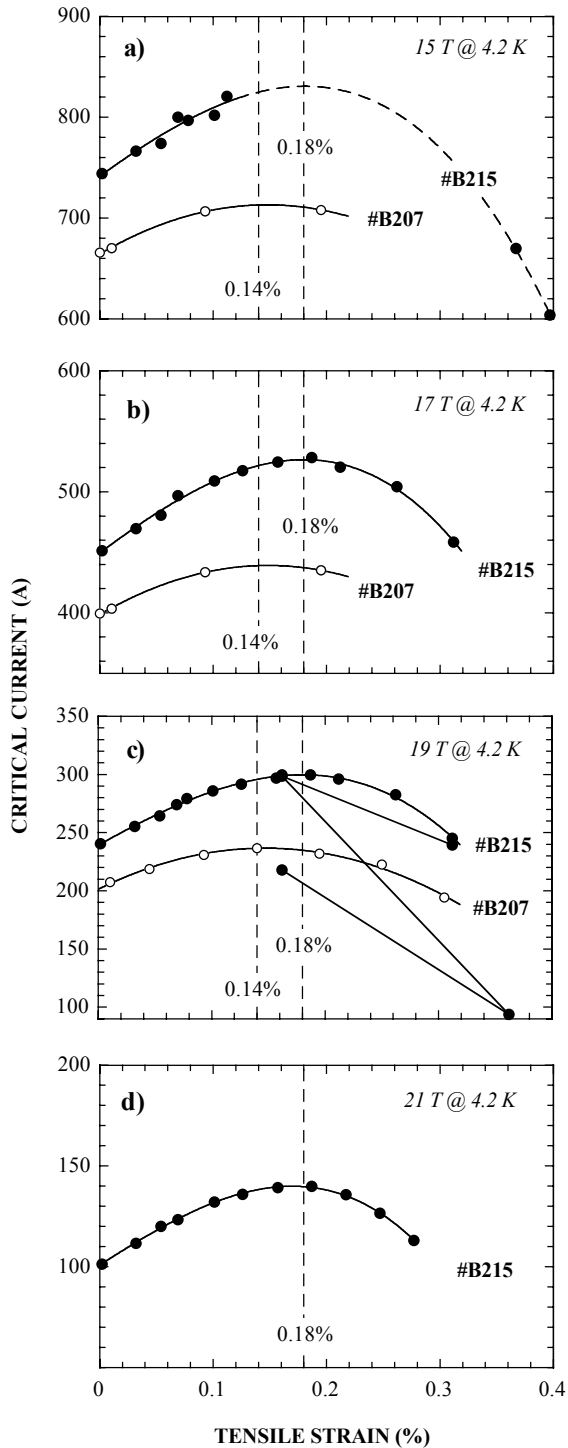


Figure 4. Critical current ( $0.1 \mu\text{V}/\text{cm}$ ) as a function of axial tensile strain at different magnetic fields.

strain. A Kramer extrapolation at zero tensile strain yields a  $B_{c2}(4.2 \text{ K})$  of 24.8 T and 25.0 T for wire #B207 and #B215, respectively. These values increase at  $\epsilon_m$  to 25.0 T and 25.8 T, respectively.

### Critical current vs. transverse compressive force

Superconducting wires (strands) within a cable are subject to bending and pinching (transverse compressive stress) [5], [6]. The degradation of  $I_c$  depends on the cable pattern and of the sensitivity of the  $\text{Nb}_3\text{Sn}$  wires submitted to mechanical loads. Stress sensitivity, an inherent property of  $\text{Nb}_3\text{Sn}$ , can substantially be influenced by the layout of the wire, which is different for the known manufacturing processes (bronze route, internal tin route or powder in tube/PIT). The behaviour under bending conditions can in principle be estimated from  $I_c$  vs. axial tensile strain/stress measurements [7], while the determination of pinching effects requires a specially designed experimental setup.

We have developed a new probe allowing the study of the critical current as a function of transverse compressive forces up to 40 kN in magnetic fields up to 21 T [8]. The gauge length over which the transverse force is applied is 120 mm thus allowing the application of very low voltage criteria as well as the study of the influence of the twist pitch length. In Fig. 5 the critical current vs. transverse compressive force at various fields for wire #B215 is shown. The behaviour is very similar to that of wire #B207 [9]. The field dependence can be seen more clearly in Fig. 6 where the normalized critical current  $I_c/I_{c0}$  is plotted against the transverse compressive force. Note that the main difference appears at forces below 2 to

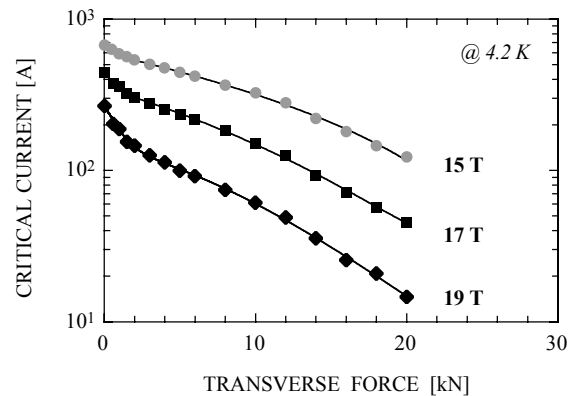


Figure 5. Critical current ( $0.1 \mu\text{V}/\text{cm}$ ) vs. transverse compressive force at different magnetic fields for wire #B215.

3 kN. This range of forces is linked to a strong reduction of the Kramer  $B_{c2}(4.2\text{K})$ .

The reversible/irreversible behaviour of  $I_c$  after unloading has been studied too. Because irreversibility

does not depend of the applied magnetic field, measurements have been carried out at 19 T. The result is summarized in Fig. 7. The data for unloading have been obtained as follows: after application of the indicated transverse compressive force (abscissa) the force was removed and the critical current was measured. Note that the critical current already shows an irreversible

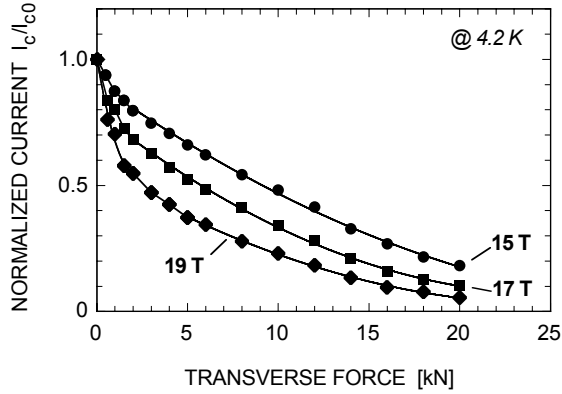


Figure 6. Normalized critical current  $I_c/I_{c0}$  as a function of transverse compressive force at different magnetic fields for wire #B215.

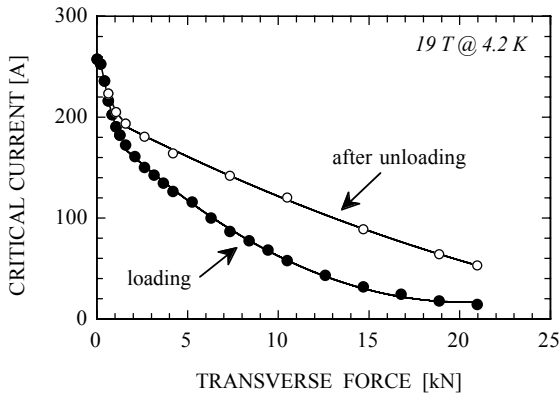


Figure 7. Critical current ( $0.1 \mu\text{V}/\text{cm}$ ) vs. transverse compressive force of wire #B215 for loading and unloading. The values for unloading are measured after removing the force (x-axis) thus indicating partial recovery.

behaviour for forces as small as 1 kN and recovers only partially for higher forces.

## DISCUSSION

It is interesting to note that the relatively small difference in the distribution of  $T_c$  between #B207 and #B215 has a rather important consequence for the critical current. First, it has been seen by specific heat that the volume fraction of  $\text{Nb}_3\text{Sn}$  in wire #B215 is about 5%

higher. Second, the  $T_c$  distribution of #B215 is smaller and the position of the peak at higher temperature. It is expected that a smaller distribution of  $T_c$  gives a smaller distribution of  $B_{c2}$ , although the situation is complicated by the observation of T. Orlando et al. that the highest  $T_c$  material does not have the highest  $B_{c2}$  [10]. In any case an average  $B_{c2}$  enters in the temperature scaling law of  $\text{Nb}_3\text{Sn}$ .

$$J_c B = C B_{c2}^{2.5} b^{0.5} (1-b)^2 \quad (2)$$

where  $J_c$  is the current density,  $B$  is the applied magnetic field,  $C$  is a constant and  $b$  is the reduced field  $B/B_{c2}$ . So a slightly higher  $B_{c2}$ , as it has been observed for #B215, contributes to a higher  $I_c$ .

The different  $\varepsilon_m$  values may come from the various Cu/non-Cu fractions. Wire #B215 has a measured Cu/non-Cu area of 1.22 (0.96 for #B207). In addition, the amount of unreacted Nb surrounding the  $\text{Nb}_3\text{Sn}$  filaments may also play a role. In fact the specific heat measurements reveal a higher volume fraction of unreacted Nb in wire #B207. Because the thermal contraction of Nb at 4.2 K is relatively small in comparison to that of  $\text{Nb}_3\text{Sn}$ , a higher volume fraction of Nb decreases the thermal prestrain exerted by the copper matrix.

Inspecting Fig. 6 the rate of degradation of the normalized critical current depends strongly of the magnetic field but only for transverse forces  $< 2$  kN. The higher the field the more sensitive is  $I_c$  against a transverse force. At higher forces the rate is almost independent of field. It is speculated that the observed behaviour is related to the Kramer  $B_{c2}$  of undamaged filaments. Actually there is a particularly strong reduction of  $B_{c2}$  (4.2 K) between zero and 2 – 3 kN transverse force which flattens at higher forces. A similar situation has been observed in wire #B207 [9].

Finally Fig. 7 indicates that permanent damage of filaments already occurs at transverse forces as low as 1 kN, while for higher forces a partial recovery is observed. Farinon et al. have shown that at room temperature in a round wire there are two conical zones, parallel to the transverse force, where filaments are deformed [11]. With increasing deformation cracks appear parallel to the force. Assuming a similar situation at 4.2 K and taking into account the twist pitch length of 20 mm, every filament of the strand is exposed several times to deformation and breakage over the gauge length of 120 mm where the transverse compressive force is applied.

Comparing the obtained results for the PIT  $\text{Nb}_3\text{Sn}$  wire with a bronze route wire reveals that the degradation of  $I_c$  is much less pronounced in the bronze route conductor [12]. At 19 T a force of 10 kN reduces the critical current to 23% of  $I_{c0}$  for the #B215 wire, compared to 60% of  $I_{c0}$  for the bronze wire. At the relevant field for NED, 15 T, these values are 48% and 80% of  $I_{c0}$ , respectively.

## CONCLUSION

In this work it has been shown that the quality of the powder ( $T_c$  distribution) plays an important role for the critical current performance of PIT wires. This was observed not only near zero axial tensile strain but also at higher strain values, in particular at  $\varepsilon_m$ . With respect to bronze route and internal tin Nb<sub>3</sub>Sn conductors the measured  $\varepsilon_m$  is relatively low, indicating a reduced thermal prestrain.

The present layout of PIT Nb<sub>3</sub>Sn conductors was found to be extremely sensitive to transverse compressive forces. This sensitivity is enhanced with increasing magnetic fields. There is some recovery of  $I_c$  upon unloading but most of the conductor filaments are damaged. This is presumably due to the rather big size of the filaments and to the presence of voids (porosity).

## ACKNOWLEDGMENT

The authors thank Ph. Lebrun and D. Leroy from CERN for their initiative and continuous encouragement of this work. In particular we thank A. Ferreira, R. Modoux, R. Pellet and D. Zurmühle for their excellent technical assistance.

## REFERENCES

- [1] C. Senatore, D. Uglietti, V. Abächerli, A. Junod, R. Flükiger, "Specific heat, a method to determine the  $T_c$  distribution in industrial Nb<sub>3</sub>Sn wires prepared by various techniques", *IEEE Trans. Appl. Supercond.*, 17 (2007), 2611.
- [2] D. Sanchez, A. Junod, J.-Y. Genoud, T. Graf, and J. Muller, "Low-temperature specific heat of the 123, 124 and 247 phases of Y-Ba-Cu-O in magnetic fields up to 14 Tesla", *Physica C*, 200 (1992), 1.
- [3] M. Suenaga, D. O. Welch, R. L. Sabatini, O. F. Kammerer, and S. Okuda, "Superconducting critical-temperatures, critical magnetic-fields, lattice-parameters, and chemical-compositions of bulk pure and alloyed Nb<sub>3</sub>Sn produced by the bronze process", *J. Appl. Phys.*, 59 (1986), 840.
- [4] B. Seeber, D. Uglietti, V. Abächerli, P.-A. Bovier, D. Eckert, G. Kübler, P. Lezza, A. Pollini and R. Flükiger, "Critical current versus strain measurement up to 21 T and 1000 A of long length superconducting wires and tapes", *Rev. Sci. Instrum.*, 76 (2005), 093901.
- [5] N. Mitchell, "Comparison between predictions and measurements of the superconducting performance of Nb<sub>3</sub>Sn cable in conduit conductors with transverse load degradation", *Supercond. Sci. Technol.* 21 (2008), 054005.
- [6] A. Nijhuis, Y. Ilyin and W. A. J. Wessel, "Spatial periodic contact stress and critical current of a Nb<sub>3</sub>Sn strand measured in TARSIS", *Supercond. Sci. Technol.* 19 (2006), 1089.
- [7] J. W. Ekin, "Mechanical properties and strain effects in superconductors", in *Superconductor Material Science: Metallurgy, Fabrication and Applications* (S. Foner and B. B. Schwartz, eds.), New York, Plenum (1981), 455.
- [8] B. Seeber, A. Ferreira, V. Abächerli, T. Boutboul, L. Oberli and R. Flükiger, "Transport properties up to 1000 A of Nb<sub>3</sub>Sn wires under transverse compressive stress", *IEEE Trans. Appl. Supercond.*, 17 (2007), 2643.
- [9] B. Seeber, A. Ferreira, F. Buta, C. Senatore, T. Boutboul, L. Oberli and R. Flükiger, "Transport properties of a PIT Nb<sub>3</sub>Sn strand under transverse compressive and axial tensile stress", *IEEE Trans. Appl. Supercond.*, 18 (2008), 976.
- [10] T. P. Orlando, J. A. Alexander, S. J. Bending, J. Kwo, S. J. Poon, R. H. Hammond, M. R. Beasley, E. J. McNiff and S. Foner, "The role of disorder in maximizing the upper critical field in the Nb-Sn system", *IEEE Trans. MAG-17* (1981), 368.
- [11] S. Farinon, T. Boutboul, A. Devred, P. Fabbriatore, D. Leroy and L. Oberli, "FE model to study the deformation of Nb<sub>3</sub>Sn wires for the Next European Dipole (NED)", *IEEE Trans. Appl. Supercond.*, 17 (2007), 1136.
- [12] B. Seeber, A. Ferreira, V. Abächerli and R. Flükiger, "Critical current of a Nb<sub>3</sub>Sn bronze route conductor under uniaxial tensile and transverse compressive stress", *Supercond. Sci. Technol.*, 20, (2007), S184